



Estimation of radiation dose due to ingestion of radon in water samples of Garhwal Himalaya, India

Krishna Pal Singh¹ · Subhash Chandra¹ · Mukesh Prasad² · Abhishek Joshi³ · Ganesh Prasad⁴ · R. C. Ramola³

Received: 16 April 2023 / Accepted: 14 June 2023 / Published online: 3 July 2023
© Akadémiai Kiadó, Budapest, Hungary 2023

Abstract

The measurements of radon concentrations in drinking water sources in and around the Main Central Thrust (MCT) region in Garhwal Himalaya, India, were carried out using the scintillation detector-based SMART RnDuo technique for radiation protection purposes. Radon values in the analyzed samples were observed between 1.1 and 183.9 Bq L⁻¹ (AM = 19.7 Bq L⁻¹). Radon values in 94% of the samples were found well below the World Health Organization (WHO) reference limit. The estimated radiation doses for different age groups were found higher than the WHO safe limit of 100 μSv y⁻¹ (from all sources including radon) except for the age groups of 0–12 months infants and 1–3 years children. The results of this study may be useful for future studies on epidemiology, examining hidden faults, uranium exploration etc.

Keywords Main Central Thrust · RnDuo · Human health · Radon · Drinking water · Cancer

Introduction

Radon, with a half-life of 3.825 days, is produced in the soil or rocks by the decay of radium. It is discharged from the soil into the air, and water within the pores between soil and rock particles. Human beings are exposed to radiation due to naturally existing radioactivity in soil, groundwater, and indoor surroundings. Naturally occurring radionuclides are present in the earth's crust and decompose into the daughter products of higher radioactivity and shorter half-life. Most of the natural radiation exposure experienced by humans is caused due to radioactive gas radon [1, 2]. The radon gas from water reached the human body through two potential routes. Firstly, radon that has been dissolved in water can directly give doses to the body by going into the gastrointestinal tract via the ingestion route and secondly, the dissolved radon can leak out from the

household water (showering, washing clothes, flushing the toilet, and other common activities) and concentrate in confined places after that it can enter the respiratory system by inhalation process. Because of this, residents may be at risk for health problems from ingestion and inhalation of radon gas from the water [3, 4]. The amount of radon gas depends on the transportation processes from the soil matrix to the earth's environment. The transport of radon gas from mineral grains to pore spaces is governed by processes known as diffusion and advection until it eventually decays into daughter products or is exhaled into the atmosphere [5]. Diffusion is one of the primary processes through which radon enters the atmosphere. The primary source of natural radiation exposure for people is radon, which has been identified as a carcinogenic gas [6, 7]. Radon migration in the porous medium is often characterized quantitatively using the diffusion coefficient of the medium, which is directly influenced by the amount at which radon gas escapes from a porous material. The process of radon diffusion is controlled by the gradient in radon gas concentration between radon gas sources (rocks, soils, building materials, and other materials) and the ambient air. The radon diffusion coefficient can be used to ascertain various characteristics of a substance that relate to radon. The fundamental idea behind radon concentration measurement is to see how radon diffuses through the porous media. Still, some factors affect the radon diffusion coefficient, such as porosity, moisture content, tortuosity, and temperature [8, 9]. The radon concentration varies

✉ Krishna Pal Singh
krishnapalnegi@gmail.com

¹ Department of Physics, P.N.G. Govt. P.G. College, Ramnagar 244715, India

² School of Engineering and Technology, Chitkara University, Solan, Himachal Pradesh 174103, India

³ Department of Physics, H.N.B. Garhwal University, Badshahi Thaul Campus, Tehri Garhwal 249199, India

⁴ Department of Physics, B.L.J. Govt. P.G. College, Purola, Uttarkashi 249185, India

from place to place due to the geological changes in the different areas [10]. Still, in the groundwater, the primary source of it is the presence of radium and uranium-bearing elements in rock and soil [11, 12].

Radium and uranium are responsible for the high radon concentration in the soil and water sources. The concentration of radium and uranium changes with the geology of different regions. The results of the earlier investigations also suggested that the geological formation is responsible for the variation of the radon concentration in water supply, soil particles, radionuclide distribution, gamma dose rate, and related health hazard indices [13–15]. In Garhwal Himalaya, radon and its progeny measurements in the indoor atmosphere are reported in the recent decade for radiation protection purposes [16–26]. The measurements of radon and thoron exhalation rates in the soil samples and soil gas radon concentrations in the Himalayan regions of Uttarakhand state [27–31]. Radionuclide content and Gamma dose rate in the Budhakedar region lying along the MCT were found to be significantly higher than the Indian and global average values [32–38]. However, for the Ukhimath region, which also lies along the MCT, natural radioactivity level, radium content, various hazard indices, and annual gamma dose rate were found within the safe limit [39]. It is also found that the occurrence of high values of radon concentration in the groundwater source is related to the regions with radium or uranium-bearing granitic rocks. The presence of active thrusts, faults, shears and displacement of cracks that takes place in regions near active faults enables the upward migration of radon gas [40, 41]. The geohydrology (fault–lineament (FL) and fracture–joint (FJ) type springs) plays an important role in the occurrence of elevated radon levels in groundwater [42, 43]. However, a few studies have been carried out on radon and uranium measurements in drinking water sources [38, 43, 44]. On the other hand, relatively low radon values in the groundwater sources were observed in sedimentary rocks or soil regions [43]. In the present study, in situ, measurements of radon concentrations were carried out in different types of water sources such as springs, taps, and handpump in and around the Main Central Thrust (MCT) in Garhwal Himalaya, India for the assessment of health risks in terms of radiological dose. It is worth highlighting that all these samples are used by the general public for drinking purposes. The results of this study may be useful for uranium exploration, hidden thrusts and faults allocation in addition to health risk assessment [45].

Materials and methods

Study area

The study region is located in the Uttarkashi district of Uttarakhand state between latitude 30.64 N to 30.90 N and

longitude 78.32° E to 78.68° E. The Uttarkashi district consists of the Lesser, Central, and Tethys Himalayas rocks. The present study area covers a few parts of the Higher Himalayas and a large part of the Lesser Himalayas region along with Main Central Thrust (MCT). This region contains a very complex geology due to repeated tectonic disturbance. It can be classified with the help of super-subsequences based on the order of occurrence of the group of rocks. In terms of super-subsequences, it is divided into six parts, viz. Archaean, Paleoproterozoic, Mesoproterozoic to Neoproterozoic, Neoproterozoic to Paleozoic, Ordovician to Carboniferous, Late Permian to Late Triassic. The present study area falls under the Paleoproterozoic super-subsequence of the Garhwal group, and most of the parts of the Lesser Himalaya came under this Garhwal group. The boundary of the Garhwal group is situated by the Main Central Thrust (MCT) in the northern zone and by Main Boundary Thrust (MBT) in the southern area. The Garhwal group is exposed to two tectonic zones detached by the Vaikrita group's rocks that contact with North Almora Thrust (NAT) in the northern region and are limited to Main Boundary Thrust to South Almora Thrust (SAT) in the southern zone. The rocks in the study region are classified as quartzite, slates, phyllite, dolomite, limestone, etc. [46]. The study area was covered along and across the MCT, affected by many landslides, earthquakes, and rockfalls. The leading cause of these natural disasters is the movement of the Indian plate towards the Eurasian plate [47–49]. The unique property of this area is that new tectonic activities occasionally happen in this region, which developed several faults and weak plans that change the geology of the study area. Several other faults are present in this area besides the Main Central Thrust [27, 32, 50]. The main rocks types of the present study area (MCT) are categorized as quartzite, slates, limestone, dolomite, phyllite, meta basic, and granite etc. these rocks are intruded by acid and basic igneous rocks [46, 51]. The sampling map of the present study regions is shown in Fig. 1. The water samples were collected from the different spring sources of almost all villages of the study region. However, tap and handpump water samples were collected only from those villages where there was no spring water source for the radon concentration measurements.

Measurement of radon concentration in water

In this study, 94 water samples were taken for the investigation, of which 64 are spring water, 17 are tap water, 12 are hand pump water, and 1 is hot spring water. Among 94 investigated samples, 46 were taken along and across the MCT, and 48 were from nearby locations in the Uttarkashi district of Uttarakhand state. All the investigated water sources except the hot spring (N = 1) are used for drinking

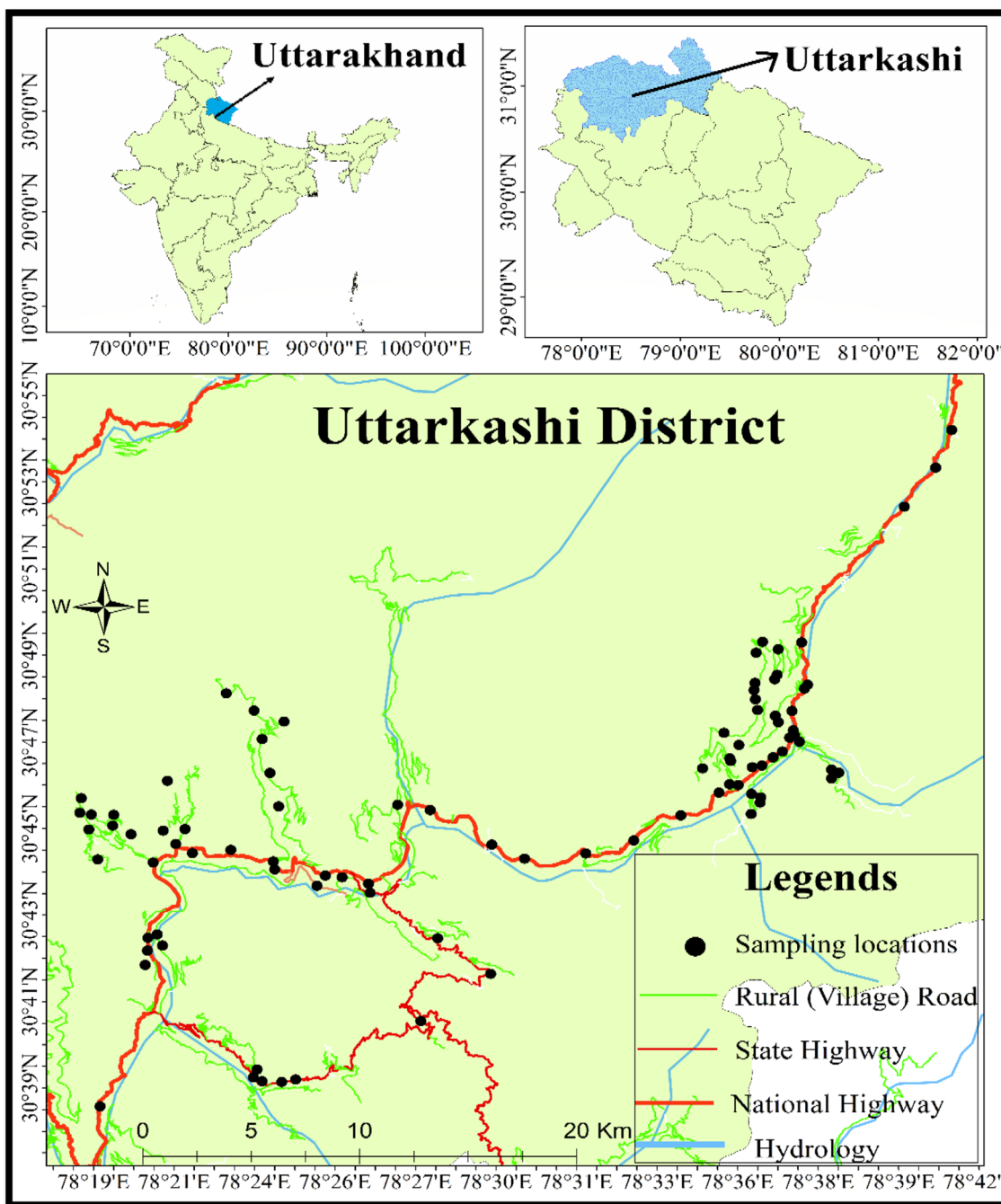


Fig. 1 The study area map shows sampling locations

by the population in the study region. The collection of the water sample was done between the month of April–May and November–December of the calendar year 2022 to avoid any contamination due to rain during monsoon. The sampling procedure and the measurement technique are discussed below.

Sampling procedure and radon measurements in water

In the present study, a scintillation principle-based detector SMART RnDuo device was used to measure radon concentration in different water samples. The water samples were collected in such a way as to minimize the aeration because

radon can rapidly escape from the water. Figure 2 shows the sampling setup of the Smart RnDuo device, a portable radon monitor connected to the bubbler kit and sampling bottles. The water samples from springs, taps, and handpumps were collected in sampling bottles from a jug filled with water to be collected for analysis (Fig. 3).

The protocols of sampling and measurement were strictly followed to investigate radon levels in water samples [52]. The radon gas is pushed out from the scintillation cell to eliminate any background radiation inside the detector volume before the actual measurement of the radon gas in the water sample using an internal pump. The connection was made so that a flexible tube attached to the bubbler kit is connected to the RnDuo monitor, as shown in Fig. 2.

Then again, ON the pump manually for 2–3 min so that the dissolved radon gas could escape into the tubing, and this was done in the closed loop. After giving a 5-min delay from the pump OFF time, measurement was started, and it was taken in 15 min-cycle for 1 h for each sample. After taking the average of these readings, we obtained radon concentration in the air as C_{air} (Bq m^{-3}), and once we obtain radon concentration in the air, we can easily calculate the radon concentration in liquid (C_{liq}) in (Bq m^{-3}) using the following Eqs. [43, 52].

$$C_{\text{liq}} = C_{\text{air}} \left(K + \frac{V_{\text{air}}}{V_{\text{liq}}} \right) \quad (1)$$

where the value of K taken for the measurement is 0.25 and known as the partition coefficient of radon in liquid to air, V_{air} is closed loop total air volume of the setup [detector volume + tubing volume + bubbler kit volume] (ml), and V_{liq} is the liquid volume in the sampling bottles (ml). The value taken for the measurement in this paper for V_{air} is 262 ml and V_{liq} is 30 ml.

Dose assessment

There are two processes by which radon enters the human body from the water, i.e. ingestion of drinking water and inhalation of radon released from household water to the indoor air. The inhalation of radon is considered to cause respiratory problems in human beings.

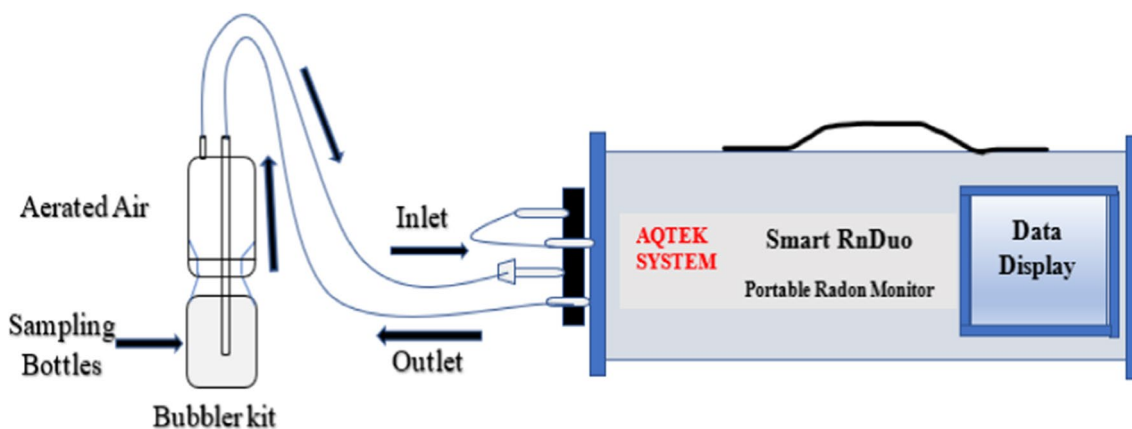
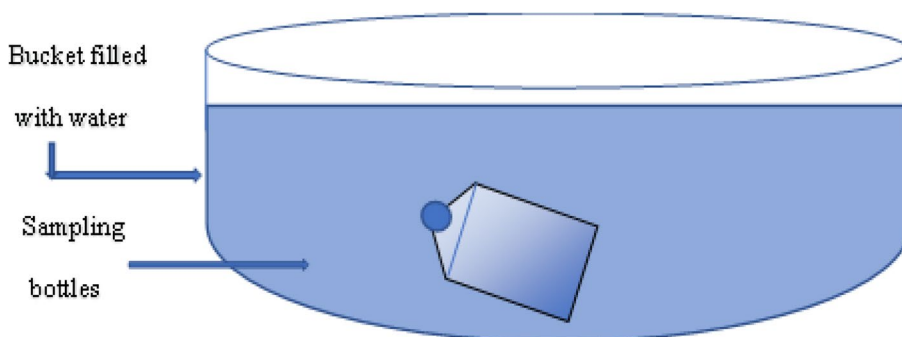


Fig. 2 Experimental setup for the measurement of radon in water

Fig. 3 Method of water sample collection



Age-dependent dose assessment from ingestion of water

The ingestion dose from radon concentration in drinking water samples for individuals of different age groups in different life stages was calculated from the following equation [53].

$$D_{\text{Ing}} = C_{\text{liq}} \times \text{DWI} \times T \times \text{DCF} \quad (2)$$

where D_{Ing} is known as the annual effective dose due to the ingestion of radon gas in drinking water and calculated in μSvy^{-1} , C_{liq} is the concentration of the radon gas in the water samples (Bq L^{-1}), DWI is the daily water intake capacity from the inhabitant and its value is given in Table 1, DCF is the conversion factor for the dose ($10^{-8} \text{ Sv Bq}^{-1}$), and T is the exposure time (i.e. 365 days y^{-1}).

Inhalation dose assessment

The inhalation dose due to radon released from domestic use water to the indoor air environment was calculated from the following equation [54].

$$D_{\text{Inh}} = C_{\text{liq}} \times \frac{R_a}{R_w} \times \text{EF} \times T_i \times 8760 \times \text{DCF} \quad (3)$$

where D_{inh} is the annual effective dose due to inhalation of radon escaping from the domestic use water and calculated in μSvy^{-1} , C_{liq} is the concentration of the radon gas in the water samples (Bq m^{-3}). R_w and R_a are the concentrations of radon gas in water and air, respectively ($R_a/R_w = 10^{-4}$). EF is the equilibrium factor for radon, T_i is the time spent inside the house by an individual, EF (0.42) and T_i (0.82) are

for Garhwal Himalaya regions [19, 40, 55] and DCF is the conversion factor for dose ($9 \text{ nSv Bq}^{-1} \text{ m}^3 \text{ h}^{-1}$) [56].

The annual mean effective dose (D_{Total}) was calculated for different body organs from the UNSCEAR relations [57].

$$D_{\text{Total}} = W_{\text{Tissue}} \times D(\text{Ingestion, Inhalation}) \quad (4)$$

where W_{Tissue} is the tissue weighting factor (0.12 for the lungs and stomach, 0.05 for the liver and kidney, etc.) [58], and D is the effective ingestion and inhalation dose measured separately.

Excess lifetime cancer risk (ELCR)

The Excess lifetime cancer risk (ELCR) was calculated by the following relation [58].

$$\text{ELCR} = \text{AED}(\text{Ingestion, Inhalation}) \times \text{ADL} \times \text{RF} \quad (5)$$

where AED (ingestion, inhalation) is the annual effective dose due to ingestion and inhalation of water (μSvy^{-1}), ADL is the average duration of life for the country (70 years) and RF is a risk factor (0.05 Sv^{-1}) [58].

Results and discussion

Radon concentration in the different types of water sources

Radon concentration in different water samples was analyzed in this study, and its statistical values are shown in Table 2. The radon concentration in all of the water samples ranges from 1.1 to 183.9 Bq L^{-1} with a mean value

Table 1 Annual effective ingestion and inhalation dose (μSvy^{-1})

Life stages	Age groups (DWI)	Min value	Max value	Avg value	SD	Geo mean	MCT samples (AM)	Uttarkashi samples (AM)
Infant	0–6 months (0.7)	2.85	469.76	50.27	103.47	16.90	78.94	20.71
	7–12 months (0.8)	3.25	536.87	57.45	118.25	19.31	90.22	23.67
Children	1–3 years (1.3)	5.29	872.41	93.35	192.15	31.39	146.60	38.46
	4–8 years (1.7)	6.91	1140.84	122.08	251.27	41.04	191.71	50.30
Male	9–13 years (2.4)	9.76	1610.60	172.34	354.74	57.94	270.65	71.01
	14–18 years (3.3)	13.42	2214.58	236.97	487.76	79.67	372.15	97.64
Adult	> 18 years (3.7)	15.04	2483.01	265.69	546.89	89.33	417.26	109.47
Female	9–13 years (2.1)	8.54	1409.28	150.80	310.40	50.70	236.82	62.13
	14–18 years (2.3)	9.35	1543.50	165.16	339.96	55.53	259.37	68.05
Adult	> 18 years (2.7)	10.98	1811.93	193.88	399.08	65.19	304.48	79.88
pregnancy	14–50 years (3.0)	12.20	2013.25	215.43	443.42	72.43	338.32	88.76
Lactation	14–50 years (3.8)	15.45	2550.12	272.87	561.67	91.74	428.53	112.43
$D_{\text{inhalation}}$		3.02	499.22	53.42	109.95	17.96	83.89	22.01

of 19.7 Bq L^{-1} . The pH and temperature value varies from 6.3 to 7.9 and 13.1 to 58.9°C with mean values of 7.1 and 20.3°C, respectively. The pH values and temperature (With hot spring and without hot spring) showed a negative correlation (Pearson's $r = -0.12, -0.14,$ and -0.20 respectively) to the radon activity concentration in water samples (Fig. 4).

Further, the study was categorised into two different regions to check the variation of radon concentration in their water samples and it is observed that the Main Central Thrust region has a higher radon concentration (30.9 Bq L^{-1}) than the Uttarkashi region (8.11 Bq L^{-1}) which seems to be obvious as the MCT having active thrust fault and a tectonically active zone. The average values of pH and temperature were found 6.9°C and 20.8°C, 7.2 and 20.4°C for MCT and Uttarkashi region respectively.

The source-wise comparison between springs, taps and handpumps water samples was also done in the present study for dissolved radon gas and it is found that the tap waters of the study area have higher radon concentration in comparison to the springs and handpumps water. The mean values obtained from all water samples (19.47 Bq L^{-1}), spring water samples (14.74 Bq L^{-1}), tap water samples (47.26 Bq L^{-1}) and handpump water samples (7.28 Bq L^{-1}) are given in Fig. 5 a–d respectively). There are three samples in spring water, three in tap water, and none of the samples in hand pump water exceeds the safe limit as recommended by WHO (100 Bq L^{-1}), approximately 94% of the samples are well within the safe limit.

Region-wise comparison (MCT region and Uttarkashi region) for dissolved radon gas in the water samples is

Table 2 The statistical value for Radon in air, radon in water, pH, and temperature for the study area

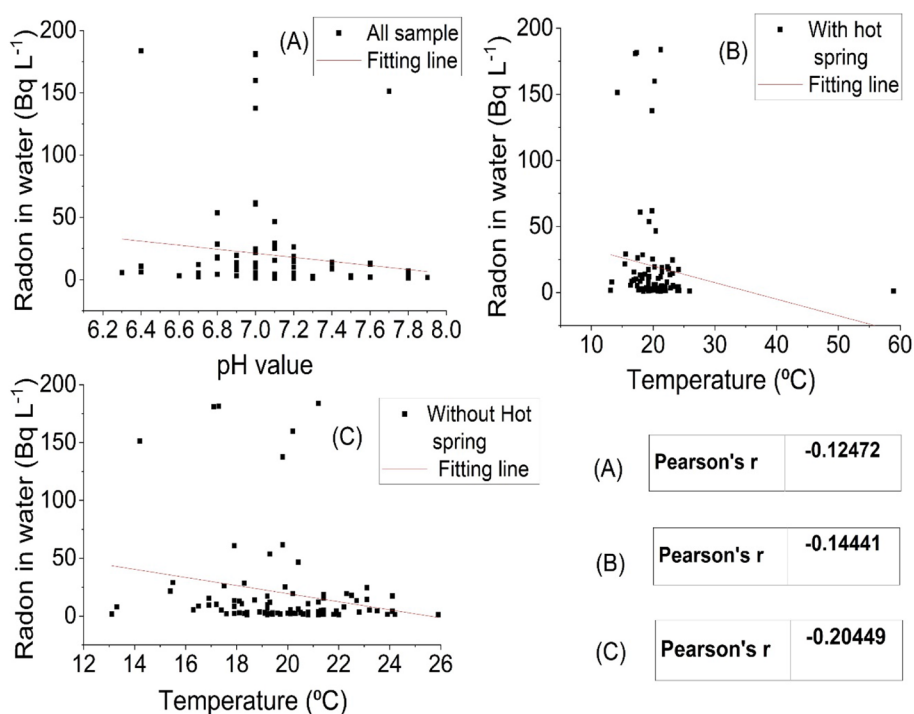
Parameters*	C_{air} (Bq m^{-3})	C_{liq} (Bq L^{-1})	pH	Temperature ($^{\circ}\text{C}$)
Min	124	1.11	6.3	13.1
Max	20,467	183.86	7.9	58.9
AM	2190	19.67	7.1	20.3
SD	4508	40.50	0.3	4.7
GM	736	6.61	7.1	19.9
AM (MCT region)	3514	30.90	6.9	20.2
AM (Uttarkashi region)	902	8.11	7.2	20.4

Min = Minimum, Max = Maximum, AM = Arithmetic Mean, SD = Standard Deviation, GM = Geometric Mean

shown in Fig. 6, and the mean value obtained is 30.9 Bq L^{-1} and 8.1 Bq L^{-1} for the Main Central Thrust samples and Uttarkashi samples respectively. It is clearly shown in Fig. 6 that the MCT region has five samples and the Uttarkashi region has only one sample that are higher values than the recommended level of 100 Bq L^{-1} by WHO and the high value in that one spring water sample (Uttarkashi region) may be due to collected from the fracture-joint rocks [43].

Figure 7 shows a box whiskers diagram of the Radon (^{222}Rn) concentration in all of the water samples. The mean value of the dataset is higher than the median and falls in the fourth quartile of the box plot. Approximately 80% of the samples had a radon concentration of less than 25 Bq L^{-1} .

Fig. 4 The correlation coefficient between Radon in water with **A** pH values, **B** temperature with a hot spring, **C** temperature without a hot spring



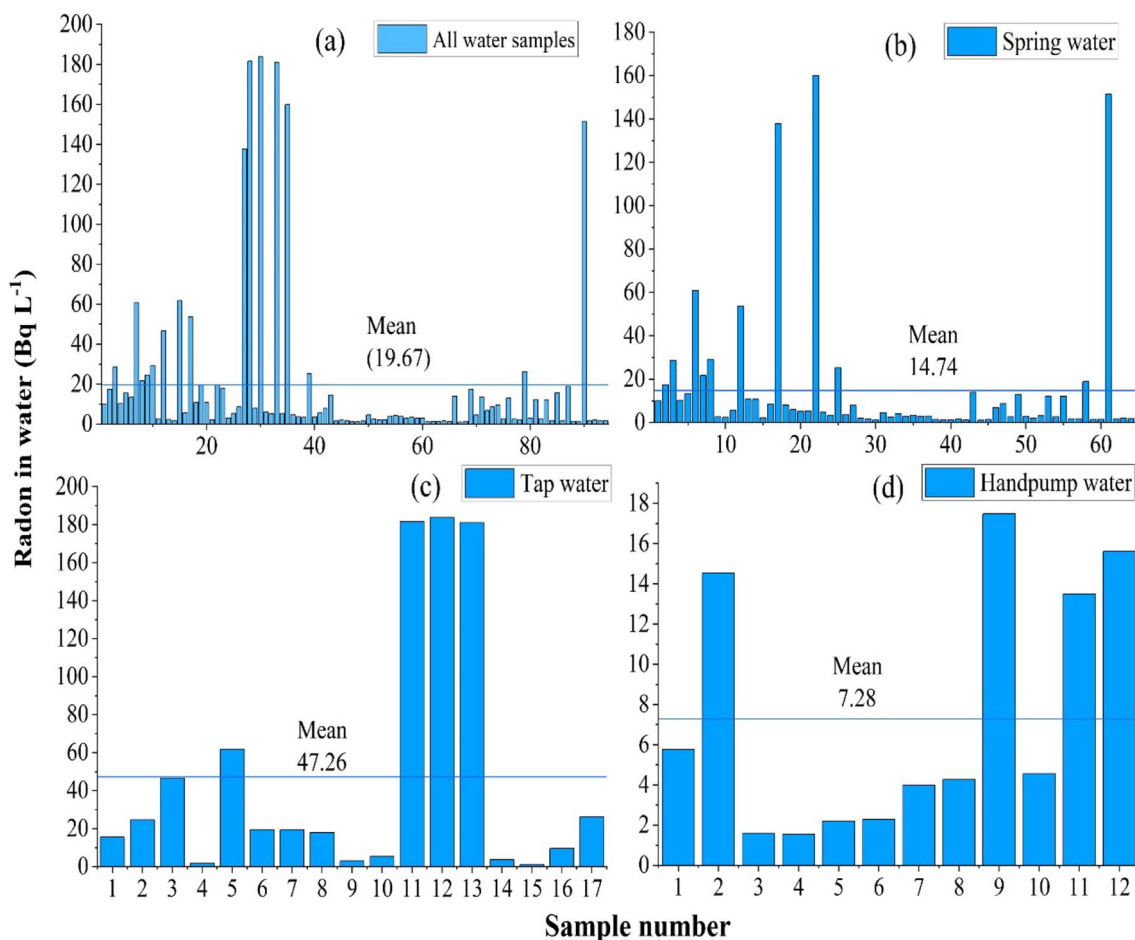


Fig. 5 Source-wise comparisons of radon concentration in water samples

Only six out of the ninety-four samples show a value of more than 100 Bq L^{-1} . The kernel density of the dataset is shown on the right side of the diagram and it can be seen that only a small percentage of the data points are situated outside the core region of the kernel density. Hence it represents the negative skewness in the dataset. The statistics show that the ^{222}Rn concentration in different water samples is widely distributed over the study area.

Spatial distribution map study

The spatial distribution curve is plotted for the measured values of radon content in water samples collected from the study area and is shown in Fig. 8. The map is separated into two parts by the marking of a red line, which is (a) the Uttarkashi region and (b) the Main Central Thrust region. An inverse distance weighted approximation is considered for the surface plot of the radon concentration in water samples. The value shown in this map is classified into nine equal interval breaks. It can be seen from the map that most of the samples are lower valued (less than 22 Bq L^{-1}) and labelled

as green-coloured surfaces. Five samples have higher values than the WHO reference level in the Main central thrust region and are labelled as red-coloured surfaces [4]. However, only one sample is higher than the reference levels in the Uttarkashi region and is labelled as pink-coloured surfaces. It can be concluded from the map that the Uttarkashi region's water is safer than the Main Central Thrust region's water for public drinking as well as health purpose.

Annual effective dose (AED)

The annual effective dose (AED) due to ingestion is calculated for the different age groups of the relative population as per their daily water intake parameter (DWI) in Table 1 [59–61]. The average value of the AED due to ingestion is found to be higher ($> 100 \mu\text{Svy}^{-1}$) in all of the age groups except 0–12 months infant and 1–3 years children. The higher average value is found in males of age groups above 18 years and lactating women (maximum in lactating women in all of the age groups) age groups due to their high daily water intake (DWI). In comparison

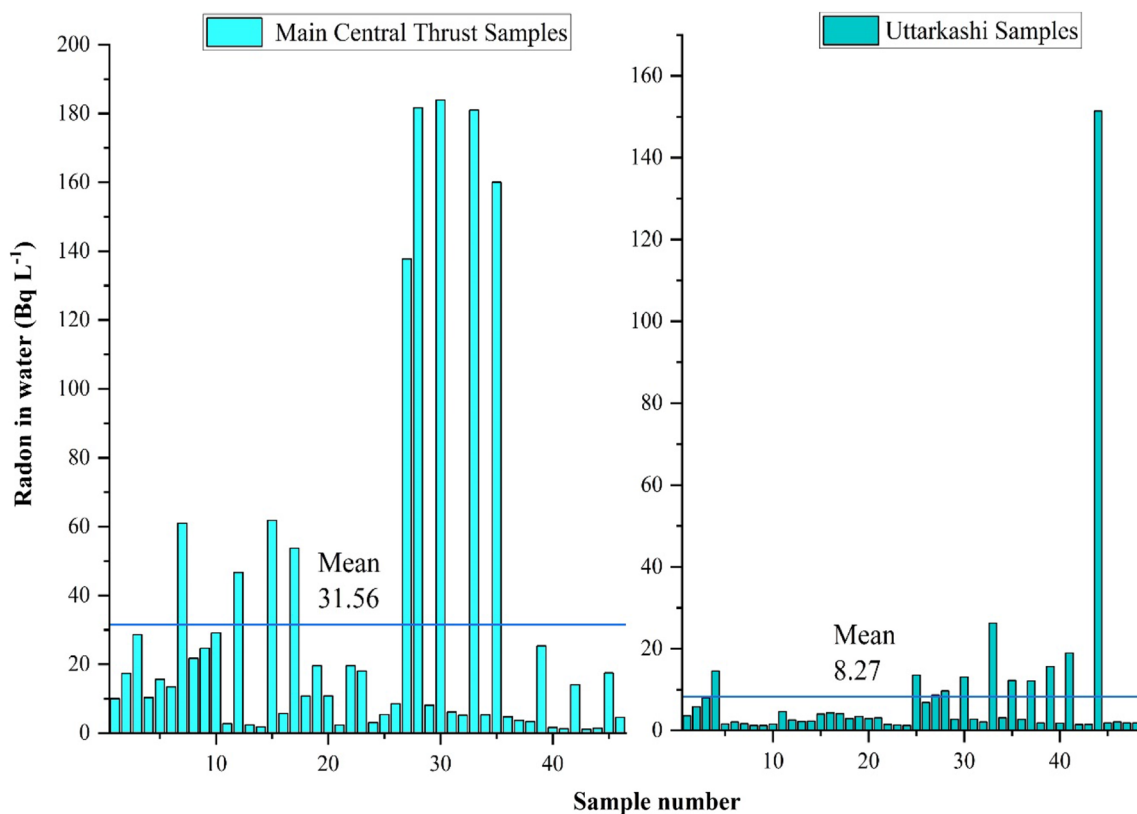
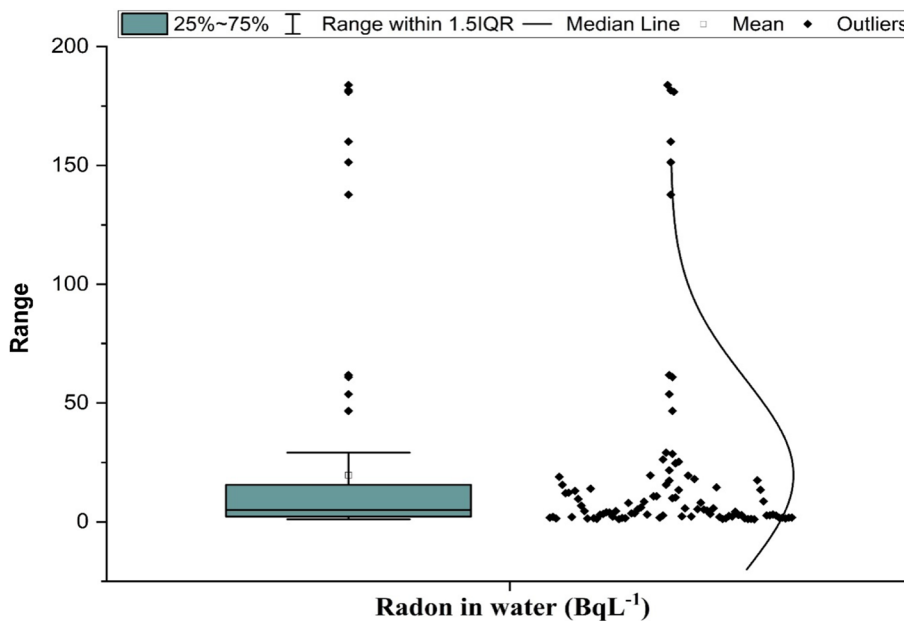


Fig. 6 Region-wise comparison of radon concentration in water samples

Fig. 7 Box plot representing statistics of radon concentration in water samples



to the overall average values, the Main Central Thrust region shows a higher average value and the Uttarkashi region shows a lower average value. The annual effective dose due to inhalation (Table 1) is found between 3.02

and 499.22 $\mu\text{Sv}\text{y}^{-1}$ with a mean value of 53.42 $\mu\text{Sv}\text{y}^{-1}$. The AED due to inhalation is found to be safe as their mean value is lower than 100 $\mu\text{Sv}\text{y}^{-1}$ in both (MCT and Uttarkashi) regions.

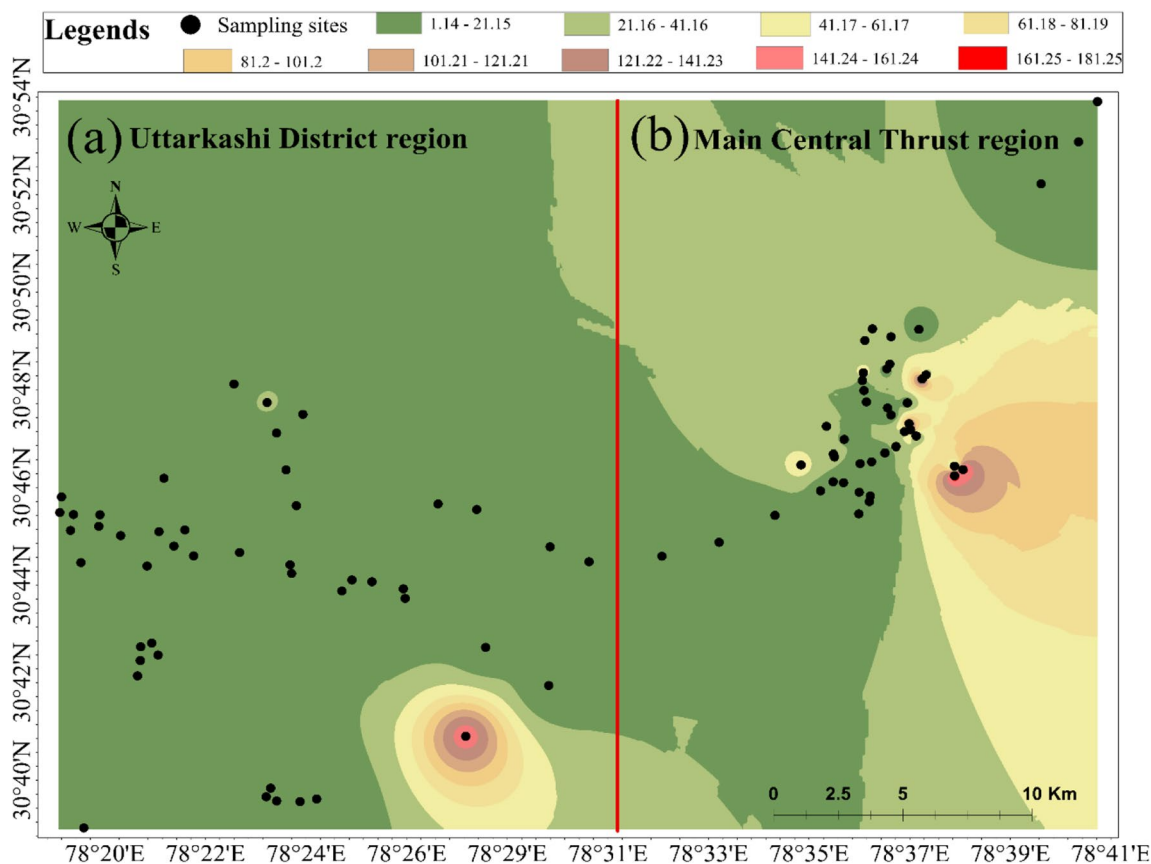


Fig. 8 Spatial distribution map for radon concentration in water samples

Annual mean effective dose (D_{total})

The estimated annual mean effective dose from the AED due to ingestion and inhalation for the lungs and stomach (Taking $W_{Tissue} = 0.12$) is shown in Table 3. It can be seen from the table that the obtained average value of the D_{total} from ingestion dose of the lung and stomach is higher than the inhalation dose except in the age group of 0–6 months infant. The average value of the annual mean effective dose from ingestion was found to increase as the age group increases, and it varies from $6.03 \mu\text{Svy}^{-1}$ for the infant of 0–6 months age group to $67.40 \mu\text{Svy}^{-1}$ for lactation. The higher average values are found in the Main Central Thrust region and the lower is in the Uttarkashi region than the overall average. The annual mean effective dose from the AED due to inhalation is found between 0.36 and $59.91 \mu\text{Svy}^{-1}$ with a mean value of $6.41 \mu\text{Svy}^{-1}$ for the lungs and stomach. The average value around Main Central Thrust and Uttarkashi regions is again higher and lower, respectively than the overall averages.

Excess lifetime cancer risk (ELCR)

The estimated values of the excess lifetime cancer risk from the AED due to ingestion and inhalation are shown in Table 4. It is concluded from the table that the ELCR for all of the age groups due to their ingestion and inhalation are within the safe limit of 1.45×10^{-3} recommended by UNSCEAR [62, 63]. The area with tectonically active (MCT) has higher values and Uttarkashi has lower than the overall average values.

Table 5 shows the comparison of the radon concentration in water samples from different countries with their different geology. The range and their mean values (which were possible) for the radon concentration in water samples are summarized with respective references. The higher value found in this table is for Kenya (371.7 Bq L^{-1}) and South Korea (300 Bq L^{-1}) respectively.

Table 3 Annual mean effective ingestion and inhalation dose for the lungs and stomach (μSvy^{-1})

Life stages	Age groups	Min value	Max value	Avg value	SD	Geo mean	MCT samples (AM)	Uttarkashi samples (AM)
Infant	0–6 month	0.34	56.37	6.03	12.42	2.03	9.68	2.54
	7–12 month	0.39	64.42	6.89	14.19	2.32	11.06	2.90
Children	1–3 year	0.63	104.69	11.20	23.06	3.77	17.97	4.71
	4–8 year	0.83	136.90	14.65	30.15	4.93	23.51	6.16
Male	9–13 year	1.17	193.27	20.68	42.57	6.95	33.18	8.70
	14–18 year	1.61	265.75	28.44	58.53	9.56	45.63	11.96
Adult	> 18 years	1.81	297.96	31.88	65.63	10.72	51.16	13.41
Female	9–13 year	1.02	169.11	18.10	37.25	6.08	29.04	7.61
	14–18 year	1.12	185.22	19.82	40.79	6.66	31.80	8.34
Adult pregnancy	> 18 years	1.32	217.43	23.27	47.89	7.82	37.33	9.79
Lactation	14–50 year	1.46	241.59	25.85	53.21	8.69	41.48	10.87
	14–50 year	1.85	306.01	32.74	67.40	11.01	52.54	13.77
$D_{\text{tot (Inh)}}$		0.36	59.91	6.41	13.19	2.16	10.29	2.70

Table 4 Excess lifetime cancer risk (ELCR) from annual effective ingestion and inhalation dose ($\times 10^{-3}$)

Life stages	Age groups	Min value	Max value	Avg value	SD	Geo mean	MCT samples (AM)	Uttarkashi samples (AM)
Infant	0–6 months	0.010	1.644	0.176	0.362	0.059	0.276	0.072
	7–12 months	0.011	1.879	0.201	0.414	0.068	0.316	0.083
Children	1–3 years	0.018	3.053	0.327	0.673	0.110	0.513	0.135
	4–8 years	0.024	3.993	0.427	0.879	0.144	0.671	0.176
Male	9–13 years	0.034	5.637	0.603	1.242	0.203	0.947	0.249
	14–18 years	0.047	7.751	0.829	1.707	0.279	1.303	0.342
Adult	> 18 years	0.053	8.691	0.930	1.914	0.313	1.460	0.383
Female	9–13 years	0.030	4.932	0.528	1.086	0.177	0.829	0.217
	14–18 years	0.033	5.402	0.578	1.190	0.194	0.908	0.238
Adult pregnancy	> 18 years	0.038	6.342	0.679	1.397	0.228	1.066	0.280
Lactation	14–50 years	0.043	7.046	0.754	1.552	0.253	1.184	0.311
	14–50 years	0.054	8.925	0.955	1.966	0.321	1.500	0.394
$\text{ELCR}_{\text{inhalation}} (\times 10^{-3})$		0.011	1.747	0.187	0.385	0.063	0.294	0.077

Conclusions

In the present study, the concentration of radon in the water samples of 94 different places from the study area ranges from 1.1 to 183.9 Bq L⁻¹ with an average value of 19.7 Bq L⁻¹. The obtained value of radon content in five water samples is higher than the alternative maximum contamination level of 148 Bq L⁻¹ as suggested by the USEPA. However, only 6.3% of the sample are excess average values as per the recommended level of the WHO and the European Commission (EC) of 100 Bq L⁻¹. Only 26.6% of the water samples exceed the maximum contamination level, and 67.03% of the samples are well below the

maximum contamination level of 11 Bq L⁻¹ as suggested by USEPA.

The annual effective dose due to the ingestion and inhalation exceeds the safe limit of 100 μSvy^{-1} (all sources including radon) for all of the age groups except the infant (0–12 months) and children (1–3 years) as proposed by the WHO. The estimated doses are found higher in the Main Central Thrust region in comparison to the Uttarkashi region therefore, the study concluded that this report must be taken into consideration before making any policies regarding radon mitigation for that specific region. The radon concentration variation levels obtained in different water sources may help examine hidden faults, thrusts, etc., and explore uranium deposits in the study area.

Table 5 Comparison of radon concentration in water samples (Bq L⁻¹) with other environments

Country	Radon concentration in water (Bq L ⁻¹)		References
	Range	Mean	
Beijing City, China	1.45–49	11.41	[64]
Brazil	0.95–36	36	[65]
Bursa, Turkey	1.46–53.64	9.28	[66]
Busan, South Korea	0–300	–	[67]
Cyprus	0.1–5	1.4	[68]
Greece	0.8–24	5.4	[69]
Kenya	0.8–371.7	–	[70]
Lebanon	0.46–49.6	–	[71]
Libya	1.02–7.26	3.46	[72]
Pakistan	0.67–1.45	1.21	[73]
Northern Rajasthan, India	0.5–85.7	9	[74]
Garhwal Himalaya, India	1.11–183.86	19.67	Present study

Acknowledgements The author acknowledges the Uttarakhand State Council for Science and Technology (UCOST), Dehradun, Uttarakhand, India for financial support in the form of a research project. The author also extends their thanks to Nuclear Research Laboratory, H.N.B. Garhwal University, BadshahiThaul Campus, Tehri Garhwal, Uttarakhand, India extending their laboratory facilities for conducting the experimental work.

Declarations

Conflict of interest The authors declare that they don't have any conflict of interest regarding this article.

References

- WHO (2004) Guidelines for drinking-water quality, volume 1: World Health Organization, 3rd edn. WHO Library Cataloguing, Geneva
- Risk assessment (1999) Risk Assessment of Radon in drinking Water. National Academies Press, Washington, DC
- Yu KN, Guan ZJ, Stokes MJ, Young ECM (1994) A Preliminary Study on the Radon Concentrations in Water in Hong Kong and the Associated Health Effects
- World Health Organization (2017) WHO guidelines for the drinking water. World health Statistics 1–116
- Tanner AB (1980) Radon migration in the ground: a supplementary review. Nat Radiation Environ III 5–56
- IARC Working Group on the Evaluation of Carcinogenic Risks to Humans., International Agency for Research on Cancer, National Cancer Institute (U.S.) (1988) Man-made mineral fibres and radon. World Health Organization, International Agency for Research on Cancer
- Prasad G, Prasad Y, Gusain GS, Ramola RC (2008) Measurement of radon and thoron levels in soil, water and indoor atmosphere of Budhakedar in Garhwal Himalaya, India. Radiat Meas. <https://doi.org/10.1016/j.radmeas.2008.04.050>
- Ishimori Y, Lange K, Martin P et al (2013) Measurement and calculation of Radon releases from NORM residues. International Atomic Energy Agency Vienna International Centre, Austria, pp 1–103
- Feng S, Li C, Cui Y et al (2021) Novel method for measuring temperature-dependent diffusion coefficient of radon in porous media. Appl Radiat Isot. <https://doi.org/10.1016/j.apradiso.2020.109506>
- UNSCEAR SOURCES, EFFECTS AND RISKS OF IONIZING RADIATION United Nations Scientific Committee on the Effects of Atomic Radiation 1988 Report to the General Assembly, with annexes UNITED NATIONS. New York
- Sethy NK, Jha V, Tripathi RM (2015) Causes of emissions from agricultural residue burning in north-west India: evaluation of a technology policy response. Ann Geophys Atmos Hydros Space Sci 109:367–379. <https://doi.org/10.18520/v109/i10/1855-1859>
- Srilatha MC, Sannappa J, Rangaswami DR (2014) Studies on concentration of Radon and Physicochemical parameters in ground water around Ramanagara and Tumkur districts, Karnataka, India. Int J Adv Sci Tech Res 2:641–660
- Yadav M, Jindal MK, Ramola RC (2023) Study of Radionuclides in Rocks samples from Ukhimath Area and its correlation with soil and Water Data. Chemistry Africa. <https://doi.org/10.1007/s42250-023-00635-1>
- Gusain GS, Badoni M, Prasad G et al (2009) Studies of natural radionuclides and dose estimation from soil samples of Kumaun Himalaya, India. Indian J Phys 83:1215–1220. <https://doi.org/10.1007/s12648-009-0104-1>
- Gusain GS, Rautela BS, Sahoo SK et al (2012) Distribution of terrestrial gamma radiation dose rate in the eastern coastal area of Odisha, India. Radiat Prot Dosimetry 152:42–45. <https://doi.org/10.1093/rpd/ncs148>
- Ramola RC, Prasad M, Rawat M et al (2015) Comparative study of various techniques for environmental radon, thoron and progeny measurements. Radiat Prot Dosimetry 167:22–28. <https://doi.org/10.1093/rpd/ncv215>
- Prasad M, Rawat M, Dangwal A et al (2015) Measurements of radon and thoron progeny concentrations in dwellings of Tehri Garhwal, India, using LR-115 deposition-based DTPS/DRPS technique. Radiat Prot Dosimetry 167:102–106. <https://doi.org/10.1093/rpd/ncv224>
- Prasad M, Rawat M, Dangwal A et al (2016) Variability of radon and thoron equilibrium factors in indoor environment of Garhwal Himalaya. J Environ Radioact. <https://doi.org/10.1016/j.jenvrad.2015.10.017>
- Ramola RC, Prasad M, Kandari T et al (2016) Dose estimation derived from the exposure to radon, thoron and their progeny in the indoor environment. Sci Rep. <https://doi.org/10.1038/srep31061>
- Kandari T, Aswal S, Prasad M et al (2016) Estimation of annual effective dose from radon concentration along Main Boundary Thrust (MBT) in Garhwal Himalaya. J Radiat Res Appl Sci 9:228–233. <https://doi.org/10.1016/j.jrras.2015.10.005>
- Kandari T, Aswal S, Prasad M et al (2016) Study of radiation exposure due to radon, thoron and their progeny in the indoor environment of Rajpur region of Uttarakhand Himalaya. Radiat Prot Dosimetry. <https://doi.org/10.1093/rpd/ncw059>
- Pant P, Kandari T, Prasad M, Ramola RC (2016) A comparative study of diurnal variation of radon and thoron concentrations in indoor environment. Radiat Prot Dosimetry 171:212–216. <https://doi.org/10.1093/rpd/ncw061>
- Prasad M, Rawat M, Dangwal A et al (2016) Study of radiation exposure due to radon, thoron and progeny in the indoor environment of Yamuna and tons valleys of Garhwal Himalaya. Radiat Prot Dosimetry 171:187–191. <https://doi.org/10.1093/rpd/ncw055>
- Prasad M, Bossew P, Anil Kumar G et al (2018) Dose assessment from the exposure to attached and unattached progeny of radon

- and thoron in indoor environment. *Acta Geophys.* <https://doi.org/10.1007/s11600-018-0111-8>
25. Pant P, Kandari T, Prasad M et al (2018) Continuous measurement of equilibrium equivalent radon/thoron concentration using time-integrated flow-mode grab sampler. *Acta Geophys.* <https://doi.org/10.1007/s11600-018-0163-9>
 26. Ramola RC, Prasad M (2020) Significance of thoron measurements in indoor environment. *J Environ Radioact.* <https://doi.org/10.1016/j.jenvrad.2020.106453>
 27. Bourai AA, Aswal S, Dangwal A et al (2013) Measurements of radon flux and soil-gas radon concentration along the Main Central Thrust, Garhwal Himalaya, using SRM and RAD7 detectors. *Acta Geophys* 61:950–957. <https://doi.org/10.2478/s11600-013-0132-2>
 28. Yadav M, Prasad M, Joshi V et al (2016) A comparative study of radium content and radon exhalation rate from soil samples using active and passive techniques. *Radiat Prot Dosimetry* 171:254–256. <https://doi.org/10.1093/rpd/ncw069>
 29. Kandari T, Prasad M, Pant P et al (2018) Study of radon flux and natural radionuclides (226Ra, 232Th and 40K) in the Main Boundary Thrust region of Garhwal Himalaya. *Acta Geophys* 66:1243–1248. <https://doi.org/10.1007/s11600-018-0158-6>
 30. Kumar A, Singh P, Semwal P et al (2021) Study of primordial radionuclides and radon/thoron exhalation rates in Bageshwar region of Kumaun Himalaya, India. *J Radioanal Nucl Chem* 328:1361–1367. <https://doi.org/10.1007/s10967-020-07582-y>
 31. Panwar P, Prasad M, Ramola RC (2021) Study of soil-gas and indoor radon concentration in a test village at Tehri Garhwal, India. *J Radioanal Nucl Chem.* <https://doi.org/10.1007/s10967-021-07901-x>
 32. Ramola RC, Gusain GS, Badoni M et al (2008) 226Ra, 232Th and 40K contents in soil samples from Garhwal Himalaya, India, and its radiological implications. *J Radiol Prot* 28:379–385. <https://doi.org/10.1088/0952-4746/28/3/008>
 33. Ramola RC, Prasad G, Prasad Y (2007) Radon emanation from soil and groundwater and surface gamma dose rate in Budhakedar, Garhwal Himalayas, India. *Indoor and Built Environment* 16:83–88. <https://doi.org/10.1177/1420326X06074668>
 34. Ramola RC, Prasad G (2004) A Survey of Surface γ -Dose Rate in Relation to Radon Concentrations in Soil and Spring Water at Budhakedar, Tehri Garhwal (Uttaranchal). *National Symposium On Environment*
 35. Yadav M, Rawat M, Dangwal A et al (2014) Levels and effects of natural radionuclides in soil samples of Garhwal Himalaya. *J Radioanal Nucl Chem* 302:869–873. <https://doi.org/10.1007/s10967-014-3277-9>
 36. Yadav M, Rawat M, Dangwal A et al (2015) Analysis of natural radionuclides in soil samples of Purola area of Garhwal Himalaya, India. *Radiat Prot Dosimetry* 167:215–218. <https://doi.org/10.1093/rpd/ncv247>
 37. Prasad M, Ranga V, Kumar GA, Ramola RC (2020) Radiological impact assessment of soil and groundwater of himalayan regions in Uttarakhand, India. *J Radioanal Nucl Chem* 323:1269–1282. <https://doi.org/10.1007/s10967-019-06827-9>
 38. Yadav M, Prasad M, Dutt S, Ramola RC (2022) Variation of natural radioactivity in soil and water samples of Garhwal Himalaya, India. *J Radioanal Nucl Chem.* <https://doi.org/10.1007/s10967-021-08147-3>
 39. Rautela BS, Yadav M, Bourai AA et al (2012) Study of natural radionuclide and absorbed gamma dose in ukhmath area of garhwal Himalaya, India. *Radiat Prot Dosimetry* 152:58–61. <https://doi.org/10.1093/rpd/ncs187>
 40. Choubey VM, Ramola RC (1997) Correlation between geology and radon levels in groundwater, soil and indoor air in Bhilangana Valley, Garhwal Himalaya, India. *Environ Geol* 32:258–262. <https://doi.org/10.1007/s002540050215>
 41. Sezgin Z, Yüksel N, Baykara T (2006) Preparation and characterization of polymeric micelles for solubilization of poorly soluble anticancer drugs. *Eur J Pharm Biopharm* 64:261–268. <https://doi.org/10.1016/j.ejpb.2006.06.003>
 42. Thivya C, Chidambaram S, Thilagavathi R et al (2015) Occurrence of high uranium and radon in hard rock aquifers of South India - evaluating the temporal and spatial trends. *Groundw Sustain Dev* 1:68–77. <https://doi.org/10.1016/j.gsd.2016.01.003>
 43. Prasad M, Kumar GA, Sahoo BK, Ramola RC (2018) A comprehensive study of radon levels and associated radiation doses in Himalayan groundwater. *Acta Geophys* 66:1223–1231. <https://doi.org/10.1007/s11600-018-0135-0>
 44. Prasad M, Semwal P, Panwar P et al (2022) Uranium contamination in drinking water as a health concern in Uttarakhand, India. *J Radioanal Nucl Chem.* <https://doi.org/10.1007/s10967-021-08128-6>
 45. Ravikumar P, Somashekar RK (2014) Determination of the radiation dose due to radon ingestion and inhalation. *Int J Environ Sci Technol* 11:493–508. <https://doi.org/10.1007/s13762-013-0252-x>
 46. Uttarkashi D, Uttarakhand Govt., Geology and mining unit (2020) District Survey Report, Silica Sand, Uttarkashi, Uttarakhand. Uttarkashi
 47. Bilham Roger (2004) Earthquakes in India and Himalaya: tectonics, geodesy and history. *Ann Geophys* 47:839–858
 48. Jade S, Mukul M, Bhattacharyya AK et al (2007) Estimates of interseismic deformation in Northeast India from GPS measurements. *Earth Planet Sci Lett* 263:221–234. <https://doi.org/10.1016/j.epsl.2007.08.031>
 49. Jade S, Bhatt BC, Yang Z et al (2004) GPS measurements from the Ladakh Himalaya, India: preliminary tests of plate-like or continuous deformation in Tibet. *Bull Geol Soc Am* 116:1385–1391. <https://doi.org/10.1130/B25357.1>
 50. Ramola RC, Prasad Y, Prasad G et al (2008) Soil-gas radon as seismotectonic indicator in Garhwal Himalaya. *Appl Radiat Isot.* <https://doi.org/10.1016/j.apradiso.2008.04.006>
 51. Ramola RC (2014) A study of radon exhalation rates from water samples by using Liquid Scintillation Counter
 52. Operational M (2015) Portable Radon Monitor-Smart RnDuo operational manual of Portable Radon Monitor-Smart RnDuo. *Portable Radon Monitor-Smart RnDuo CONTENT*
 53. UNSCEAR Sources and effects of ionizing radiation : United Nations Committee on the Effects of Atomic Radiation : UNSCEAR 1993 report to the General Assembly, with scientific annexes. United Nations, New York
 54. SOURCES AND EFFECTS OF IONIZING RADIATION United Nations Scientific Committee on the Effects of Atomic Radiation (2000) UNSCEAR 2000 Report to the General Assembly. SOURCES UNITED NATIONS, with Scientific Annexes VOLUME I
 55. Ramola RC (1955) Assessment of health risk due to radon and its daughter product in the lower atmosphere. *Curr Sci* 73:8–9
 56. Prasad M, Kumar GA, Sahoo SK, Ramola RC (2019) Health risks associated with the exposure to uranium and heavy metals through potable groundwater in Uttarakhand state of India. *J Radioanal Nucl Chem* 319:13–21. <https://doi.org/10.1007/s10967-018-6281-7>
 57. United Nations. Scientific Committee on the Effects of Atomic Radiation (2010) Sources and effects of ionizing radiation : United Nations Scientific Committee on the Effects of Atomic Radiation : UNSCEAR 2008 report to the General Assembly, with scientific annexes. United Nations
 58. Eckerman K, Harrison J, Menzel GH, Clement HC (2012) *Annals of the ICRP Compendium of Dose Coefficients based on ICRP Publication 60*

59. Institute of Medicine (2005) Dietary reference intakes for water, potassium, sodium, chloride, and sulfate. Washington, DC. The National Academies Press
60. Li WB, Karpas Z, Salonen L et al (2009) A compartmental model of Uranium in Human hair for protracted ingestion of natural uranium in drinking Water. *Health Phys* 96:636–645
61. Mehra R, Kaur S, Chand S et al (2021) Dosimetric assessment of primordial radionuclides in soil and groundwater of Sikar district, Rajasthan. *J Radioanal Nucl Chem* 330:1605–1620. <https://doi.org/10.1007/s10967-021-07998-0>
62. UNSCEAR SOURCES AND EFFECTS OF IONIZING RADIATION United Nations Scientific Committee on the Effects of Atomic Radiation UNSCEAR 2000 Report to the General Assembly, with Scientific Annexes VOLUME I: SOURCES UNITED NATIONS. New York
63. Taskin H, Karavus M, Ay P et al (2009) Radionuclide concentrations in soil and lifetime cancer risk due to gamma radioactivity in Kizilirmak, Turkey. *J Environ Radioact* 100:49–53. <https://doi.org/10.1016/j.jenvrad.2008.10.012>
64. Wu YY, Ma YZ, Cui HX et al (2014) Radon concentrations in drinking water in Beijing city, China and contribution to radiation dose. *Int J Environ Res Public Health* 11:11121–11131. <https://doi.org/10.3390/ijerph11111121>
65. Marques AL, Dos Santos W, Geraldo LP (2004) Direct measurements of radon activity in water from various natural sources using nuclear track detectors. *Appl Radiat Isot* 60:801–804. <https://doi.org/10.1016/j.apradiso.2004.01.015>
66. Akar Tarim U, Gurler O, Akkaya G et al (2012) Evaluation of radon concentration in well and tap waters in Bursa, Turkey. *Radiat Prot Dosimetry* 150:207–212. <https://doi.org/10.1093/rpd/ncr394>
67. Cho JS, Ahn JK, Kim HC, Lee DW (2004) Radon concentrations in groundwater in Busan measured with a liquid scintillation counter method. *J Environ Radioact* 75:105–112. <https://doi.org/10.1016/j.jenvrad.2003.06.002>
68. Sarrou I, Pashalidis I (2003) Radon levels in Cyprus. *J Environ Radioact* 68:269–277. [https://doi.org/10.1016/S0265-931X\(03\)00066-3](https://doi.org/10.1016/S0265-931X(03)00066-3)
69. Nikolopoulos D, Louizi A (2008) Study of indoor radon and radon in drinking water in Greece and Cyprus: implications to exposure and dose. *Radiat Meas* 43:1305–1314. <https://doi.org/10.1016/j.radmeas.2008.03.043>
70. Otwoma D, Mustaphai A (1998) 0 Note MEASUREMENT OF ²²²Rn CONCENTRATION IN KENYAN GROUNDWATER
71. Abdallah SM, Habib RR, Nuwayhid RY et al (2007) Radon measurements in well and spring water in Lebanon. *Radiat Meas* 42:298–303. <https://doi.org/10.1016/j.radmeas.2006.11.004>
72. Amin RM (2014) IPA-Under Creative Commons license 3.0 evaluation of radon gas concentration in the drinking water and dwellings of south-west Libya, using CR-39 detectors. *Int J Environ Sci*. <https://doi.org/10.6088/ijes.20140400005>
73. Nasir T, Shah M (2012) Measurement of Annual effective doses of Radon from drinking Water and Dwellings by CR-39 track detectors in Kulachi City of Pakistan. *J Basic Appl Sci* 8:528–536
74. Rani A, Mehra R, Duggal V (2013) Radon monitoring in groundwater samples from some areas of northern Rajasthan, India, using a RAD7 detector. *Radiat Prot Dosimetry* 153:496–501. <https://doi.org/10.1093/rpd/ncs130>

Publisher's Note Springer Nature remains neutral with regard to jurisdictional claims in published maps and institutional affiliations.

Springer Nature or its licensor (e.g. a society or other partner) holds exclusive rights to this article under a publishing agreement with the author(s) or other rightsholder(s); author self-archiving of the accepted manuscript version of this article is solely governed by the terms of such publishing agreement and applicable law.